Paper

Cite this: New J. Chem., 2021, 45, 8755

Heterodinuclear [Co-Ln] complexes of semicarbazide-arm bearing ligand: synthesis from the cleavage of starting [Co-Co] complex, structures and magnetic properties

Mousumi Biswas,[a] Dipmalya Basak,[a] E. Carolina Sanudo[bc] and Debashis Ray*[a]

Received 26th February 2021,
Accepted 13th April 2021

DOI: 10.1039/d1nj00971k

Introduction

The identification of a particular ligand type for the incorporation of two different types of metal ions (3d and 4f), having varying coordination demands, within a single ligand frame is crucial for synthetic chemists to obtain heterodinuclear (3d–4f) compounds. The presence of 4f ions in such compounds modulates the overall electronic and magnetic properties while showing usually small ligand fields but large spin–orbit coupling effects.[1] Their outsized coordination numbers, adaptable coordination geometry and preference for hard donor ligands in the trivalent state make them interesting partners for the synthesis of a new and exotic family of 3d–4f complexes. This field has gained enormous interest following the discovery of ferromagnetic interactions between chosen bivalent 3d and trivalent 4f ions,[2] wherein the synthesized species could be characterized for their high spin ground state and negative axial anisotropy.[3] The theme has attracted attention in recent years owing to their fascinating molecular structures, varied amount of distortion in coordination geometry and interesting physical properties such as single-molecule magnet (SMM) behavior.[4] In recent past, such a family of molecular materials have shown potential applications in high-density magnetic data storage,[5] spintronics,[6] quantum computation,[7] homogeneous catalysis[8] and magnetic refrigeration.[9] Thus, the design and synthesis of a new ligand system would be an integral part in this endeavor of obtaining stable 3d–4f aggregates as end products. These species can have unique bridging connections, coordinated end groups and newer topology, which, in turn, could provide a unique opportunity to probe the relaxation dynamics within the aggregates. The aggregates having a fewer number of 3d and 4f ions are important for a better understanding of the 3d–4f magnetic interactions as numerous interaction pathways such as 3d–3d, 3d–4f, and 4f–4f may be operative within these compounds. Lanthanide ion–incorporated 3d–4f complexes often show increased spin ground state through d–f magnetic interactions and open up a promising avenue for interesting magnetic manifestations.[10] The best example would be the simple heterodinuclear 3d–4f complex with a permanent 3d ion for a new family of compounds through a variation of 4f ion counter parts.

Recently, we have reported a family of highly distorted dinuclear Co^{II}–Ln^{III} complexes under the coordination control of two thioether-based Schiff base anions, showing fascinating magnetic properties.[11] Now we are focused to achieve the synthesis of other families of Co^{II}–Ln^{III} complexes bound to a single ligand anion of different types, instead of two, as used in the previous case. This can also prove the feasibility for minimum number of ligand anions required to sustain the binuclear structure. The choice of the ligand anion having two different coordination pockets of varying hardness can show site-specific metal ion coordination without any coordination support from the second ligand anion and further aggregation to higher order complex formation. The availability of right number of pivalate anions in the reaction medium, preferably from starting Co_2-Piv is crucial for

[a] Department of Chemistry, Indian Institute of Technology, Kharagpur 721 302, India. E-mail: dray@chem.iitkgp.ac.in [b] Departament de Qui´mica Inorga`nica i Orga`nica, Universitat de Barcelona, Diagonal 645, 08028 Barcelona, Spain
[c] Institut de Nanocie`ncia i Nanotecnologia, Universitat de Barcelona, (IN2UB) 08028 Barcelona, Spain

† Electronic supplementary information (ESI) available: Fig. S1–S4, shape measures calculation Tables S2 and S3, selected bond lengths and angles Tables S4 and S5, hydrogen bonding parameter Table S6, CCDC reference numbers 2064791–2064794. For ESI and crystallographic data in CIF or other electronic format see DOI: 10.1039/d1nj00971k

the formation and stabilization of the Co–Ln entity from the lone ligand anion support and without any other supporting bridges like HO or O^2. In a way, the coordination of 3d and 4f ions can avoid the facile hydrolysis path for oxidocentred minerals like core formation.[12] There are very few reports of Co–Ln dimer complexes and most of the complexes were
stabilized without hydroxy bridging.[12a,b,e] For a single N donor bearing binucleating ligand system, the two available coordination pockets can effectively be employed for trapping of 3d ion with dangling carboxylato group within the ONO bite from the cleavage of carboxylate-based 3d metal precursor and 4f ion within OO bite. The carboxylate anions such as pivalate having superior coordination potential could be useful to trap the bigger 4f ion in the adjacent pocket of the ligand of choice. Thus, the incorporation of Co^{II} ion having dangling pivalate anions can show coordinationcum-bridging via a central phenol group to attract the 4f ion and scrambling of pivalate ions available only from the Co_2-Piv precursor. The obtained pH of the reaction medium did not provide HO ions for the aggregation reaction to occur. Moreover, the available pivalate anions serve as efficient inhibitors for mineral core–like aggregation. The ligand design strategy directs the coordination of N donors to the Co^{II} ion and the adjacent phenolate-ether (OO) pocket to the 4f ions following the preference from the hard and soft acid–base (HSAB) category of donor atoms and metal ions.

Earlier 1-(2-hydroxy-3-methoxybenzylidene)semicarbazide (HL) was effectively utilized to obtain Dy_2, Zn_2Dy, Co_2Dy_2 and Ni_2Dy_2 complexes from simultaneous coordination of two ligand anions in each case (see Table S1, ESI†).[13] The simplest possible heteronuclear coordination ability of the single ligand anion L platform and the stabilization of the product in the single crystalline form was not revealed in the abovementioned literature reports. As a result, we were interested to establish the coordination power of the single ligand anion (L) for dinuclear 3d–4f complex formation in the presence of pivalate ions, preventing further aggregation in the presence of more than one ligand anion.

In this work, the coordination potential of semicarbazide tail–supported ligand 1-(2-hydroxy-3-methoxybenzylidene)semicarbazide (HL) (Scheme 1) having adjacent tridentate (ONO) and bidentate (OO) chelate bites were explored for selective coordination of Co^{II} and four different 4f ions. We report the synthesis and characterization of a m-phenoxido-bridged and semicarbazide

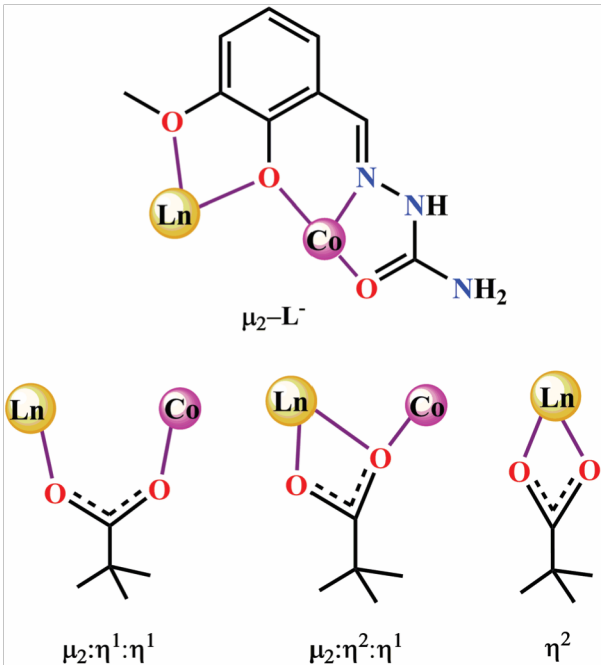

Scheme 1 Observed modes of binding of L and pivalate anions.

capped family of four dinuclear $Co^{II}Ln^{III}$ complexes $[Ln^{III}Co^{II}L(O_2CCMe_3)_4(CH_3OH)]3CH_3OH$ (Ln = Gd (1), Tb (2), Dy (3), Ho (4)). The heterometallic dinuclear aggregates of this family, assembled from the bridge cleavage of Co_2-Piv, are unknown in the literature. This encouraged us to study the importance of the ligand substitution potential for nitrates by pivalates around the 4f ions and the steric bulk on pivalate anions to restrict further aggregation toward higher order 3d–4f complexes.

Experimental section

Reagents and starting materials

Solvents and chemicals used in this work were of reagent-grade and used as received. The following chemicals were used as obtained: sodium acetate (SD Fine Chemicals, Mumbai, India); semicarbazide hydrochloride, $Gd(NO_3)_36H_2O$, $Tb(NO_3)_35H_2O$, $Dy(NO_3)_35H_2O$, and $Ho(NO_3)_35H_2O$ (Alfa Aesar, UK); $CoCO_3$, NEt_3 (SRL, Mumbai, India) and o-vanillin (Spectrochem Pvt. Ltd, Mumbai, India); MeOH (Finar Ltd, Mumbai, India); pivalic acid (Sigma Aldrich). Cobalt(II) pivalate (Co_2-Piv) salt was prepared from pivalic acid and cobalt(II) carbonate following a procedure previously reported in the literature.[14]

Synthesis of 1-(2-hydroxy-3-methoxybenzylidene)semicarbazide (HL)

The Schiff base (HL) ligand was synthesized via a direct singlestep condensation reaction with a yield of 86%, as reported earlier.[13] FT-IR and NMR spectral measurements were performed for the characterization of HL and the solid ligand was used directly for reactions with metal ion salts without further purification. Selected FT-

IR peaks (KBr disc, cm^{1}, vs = very strong, s = strong, m = medium, w = weak): 3436 (m), 3162 (m), 1664 (vs), 1600 (s), 1516 (m), 1468 (m), 1438 (m), 1351 (m), 1249 (s), 1150 (w), 1096 (m), 1075 (m), 936 (m), 782 (m), 734 (s), 570 (w), 438 (w). 1H NMR (400 MHz, DMSO-d_6, ppm): d 8.17 (1H, imineH), d 6.42 (2H, $–NH_2$), d 2.49 (1H, –NH), d 10.27 (1H, phenolic OH), d 6.42–7.37 (3H, aromatic protons), d 3.78 (3H, $–OCH_3$).

General synthetic protocols for complexes 1-4

All the metal ion complexes (1-4) were obtained by following a general synthetic procedure. To a MeOH solution of HL (0.1 mmol), another MeOH (2 mL) solution of $Ln(NO_3)_35H_2O$ (or $6H_2O$) (0.1 mmol) (Ln = Gd^{3+} (1), Tb^{3+} (2), Dy^{3+} (3) and Ho^{3+} (4)) was added followed by NEt_3 (0.2 mmol) under magnetic stirring condition to obtain a clear solution. After 1 h of stirring, a MeOH solution of Co_2-Piv (0.05 mmol) was added, and the resulting orange reaction mixture was stirred at ambient temperature for 8 h. The solution was next filtered and left undisturbed in cold place. After 2 days, orange block–shaped crystals were obtained via slow evaporation of the solvent, which were air sensitive due to loss of solvent molecules. Details for the synthesis and crystallization of the individual compounds are delineated below.

$[CoGd(L)(l_2\text{-}OOCC(CH_3)_3)_4(CH_3OH)]3CH_3OH$ (1)

The following reagents were used for the synthesis. HL (0.0209 g, 0.1 mmol), $Gd(NO_3)_36H_2O$ (0.0376 g, 0.1 mmol), Co_2-Piv (0.0474 g, 0.05 mmol), and NEt_3 (0.028 mL, 0.2 mmol). Yield: 0.040 g, 41% (based on Gd). Anal. calcd for $C_{33}H_{62}CoGdN_3O_{15}$ (957.03 g mol^{1}): C, 41.42; H, 6.53; N, 4.39. Found: C, 41.44; H, 6.54; N, 4.31. Selected IR peaks (KBr cm^{1}; s = strong, vs = very strong, m = medium, br = broad, w = weak): 2961 (br), 1661 (m), 1607 (w), 1561 (vs), 1533 (vs), 1483 (s), 1457 (m), 1420 (vs), 1360 (vs), 1219 (vs), 1154 (w), 1029 (w), 953 (w), 858 (s), 796 (m), 743 (s), 605 (s).

$[CoTb(L)(l_2\text{-}OOCC(CH_3)_3)_4(CH_3OH)]3CH_3OH$ (2)

The following reagents were used for the synthesis. HL (0.0209 g, 0.1 mmol), $Tb(NO_3)_35H_2O$ (0.0435 g, 0.1 mmol), Co_2-Piv (0.0474 g, 0.05 mmol), and NEt_3 (0.028 mL, 0.2 mmol). Yield: 0.037 g, 38% (based on Tb). Anal. Calcd for $C_{33}H_{62}CoTbN_3O_{15}$ (958.70 g mol^{1}): C, 41.34; H, 6.52; N, 4.38. Found: C, 41.29; H, 6.50; N, 4.31. Selected IR peaks (KBr cm^{1}; s = strong, vs = very strong, m = medium, br = broad, w = weak): 2961 (br), 1662 (m), 1607 (w), 1562 (vs), 1535 (vs), 1485(s), 1458 (m), 1425 (vs), 1360 (s), 1219 (vs), 1153 (w), 1029 (w), 952 (w), 897 (s), 795 (m), 745 (s), 606 (vs).

$[CoDy(L)(l_2\text{-}OOCC(CH_3)_3)_4(CH_3OH)]3CH_3OH$ (3)

The following reagents were used for the synthesis. HL (0.0209 g, 0.1 mmol), $Dy(NO_3)_35H_2O$ (0.0438 g, 0.1 mmol), Co_2-Piv (0.0474 g, 0.05 mmol), and NEt_3 (0.028 mL, 0.2 mmol). Yield: 0.035 g, 36% (based on Dy). Anal. Calcd for $C_{33}H_{62}CoDyN_3O_{15}$ (962.28 g mol^{1}): C, 41.19; H, 6.49; N, 4.37. Found: C, 41.11; H, 6.44; N, 4.34. Selected IR peaks (KBr cm^{1}; s = strong, vs = very strong, m = medium, br = broad, w = weak): 2963 (br), 1664 (m), 1608 (w), 1565 (vs), 1539(vs), 1486 (s), 1457 (m), 1427 (vs), 1361 (s), 1220 (vs), 1154 (w), 1029 (w), 953 (w), 898 (s), 796 (m), 746 (s), 608 (vs).

$[CoHo(L)(l_2\text{-}OOCC(CH_3)_3)_4(CH_3OH)]3CH_3OH$ (4)

The following reagents were used for the synthesis. HL (0.0209 g, 0.1 mmol), $Ho(NO_3)_35H_2O$ (0.0441 g, 0.1 mmol), Co_2-Piv (0.0474 g, 0.05 mmol), and NEt_3 (0.028 mL, 0.2 mmol). Yield: 0.034 g, 35% (based on Ho). Anal. Calcd for $C_{33}H_{62}CoHoN_3O_{15}$ (964.71 g mol^{1}): C, 41.09; H, 6.48; N, 4.36. Found: C, 41.01; H, 6.49; N, 4.33. Selected IR peaks (KBr cm^{1}; s = strong, vs = very strong, m = medium, br = broad, w = weak): 2963 (br), 1670 (m), 1607 (m), 1564 (vs), 1539 (vs), 1484(vs), 1457 (m), 1420 (vs), 1360 (m), 1218 (vs), 1154 (m), 1031 (m), 954 (w), 900 (w), 794 (m), 744 (s), 606 (vs).

Physical measurements

Elemental analyses (C, H, and N) of the compounds were performed using a PerkinElmer (model 240C) elemental analyzer. FTIR-ATR spectra were recorded using a Spectrometer two. Powder X-ray diffraction patterns of the complexes were obtained using a Bruker AXS X-ray diffractometer with Cu Ka radiation (l = 1.5418 Å) within a 2y range of 5–501.

Magnetic studies

Variable temperature magnetic measurements for complexes 1-4 were carried out in the Unitat de Mesures Magne`tiques (Universitat de Barcelona) on polycrystalline samples (circa 30 mg) using a Quantum Design SQUID MPMS-XL magnetometer equipped with a 5 T magnet. The dc magnetic susceptibilities were recorded at a temperature in the range of 2–300 K in a 3000 Oe dc field. Diamagnetic corrections were made using Pascal's constants and correction for the sample holder was also applied.

Single-crystal X-ray diffraction analysis

Single-crystal X-ray diffraction data for complexes 1-4 were collected using a Bruker SMART APEX-II CCD X-ray diffractometer furnished with a graphite-monochromated Mo Ka (l = 0.71073 Å) radiation using the o scan method at a temperature of 150–160 K. Data processing and space group determination were done using the SAINT[15] and XPREP[16] software. The structures of the complexes were solved by a direct method protocol of SHELXT-2014[17] and refined with full-matrix least squares against F^2 using the SHELXL (2014/7)[18] program package included in the Olex-2 software.[19] The data were corrected by empirical absorption correction using the SADABS[20] program. All non-hydrogen atoms were refined with anisotropic displacement parameters. The hydrogen atoms were incorporated at calculated positions and refined isotropically. Crystallographic diagrams were generated using the MERCURY and DIAMOND[21] software. Crystallographic data and refinement parameters for complexes are summarized in Table 1. Crystallographic data were deposited with the Cambridge Crystallographic Data Centre as supplementary publications CCDC numbers 2064791–2064794 for complexes 1-4.†

Results and discussion

Synthetic procedures

The binucleating ligand 1-(2-hydroxy-3-

Table 1 Crystal data and structure refinement summary of 1–4

	1 (Ln = Gd)	2 (Ln = Tb)	3 (Ln = Dy)	4 (Ln = Ho)
Empirical formula	$C_{33}H_{62}CoGdN_3O_{15}$	$C_{33}H_{62}CoTbN_3O_{15}$	$C_{33}H_{62}CoDyN_3O_{15}$	$C_{33}H_{62}CoHoN_3O_{15}$
Formula weight	957.03	958.70	962.28	964.71
Crystal system	Orthorhombic	Orthorhombic	Orthorhombic	Orthorhombic
Space group	$Pca2_1$	$Pca2_1$	$Pca2_1$	$Pca2_1$
a (Å)	22.46(3)	22.380(4)	22.6276(16)	22.550(5)
b (Å)	10.229(15)	10.198(2)	10.2921(7)	10.051(2)
c (Å)	18.36(3)	18.341(4)	18.4487(13)	18.174(4)
Volume (Å^3)	4219(11)	4186.0(14)	4296.4(5)	4119.1(15)
Z	4	4	4	4
D_{calcd} (g cm3)	1.507	1.521	1.488	1.556
Absorption coefficient (mm^1)	2.017	2.138	2.176	2.377
F (000)	1968	1972	1976	1980
Temperature/K	153.15	160.15	150.15	156.15
Reflections collected/unique	53366/9228	47283/7480	48312/7465	52955/8580
Limiting indices	28 r h r 26, 12 r k r 13, 23 r l r 23	26 r h r 26, 11 r k r 12, 21 r l r 21	26 r h r 26, 12 r k r 12, 21 r l r 21	28 r h r 28, 13 r k r 13, 23 r l r 21
Parameters	498	499	499	499
Goodness-of-fit (F^2)	1.072	1.072	1.096	1.058
Largest diff peak/hole (e Å^3)	0.895, 0.669	0.765, 0.637	2.514, 1.399	1.071, 0.847
R_{int}	0.0694	0.0537	0.0721	0.0474
R_1; wR_2 [I 42s(I)]	0.0383; 0.0763	0.0299; 0.0618	0.0560; 0.1411	0.0281; 0.0611
CCDC No.	2064791	2064792	2064793	2064794

methoxybenzylidene)semicarbazide (HL) is acquired following a standard Schiff base condensation reaction between semicarbazide hydrochloride and ovanillin. We were tempted to use HL in a NEt_3 medium to trap a Co^{II} ion and four other 4f ions in two adjacent and pre-assigned coordination pockets of binucleating tetradentate ligand anions. The adjacent methoxy group (–OMe) to phenoxido group is utilized to bind the Ln^{III} ions further bridged and chelated by four pivalate ions obtained from (Co_2-Piv). The stepwise addition of $Ln(NO)_3$ nH_2O (Ln = Gd^{3+}, Tb^{3+}, Dy^{3+} and Ho^{3+}) to a MeOH (4 mL) solution of HL and NEt_3 followed by Co_2-Piv in a 1:1:2:0.5 molar ratio resulted in clear orange solutions in all four cases. Roomtemperature evaporative crystallization from these solutions provided $[LnCo(L)(O_2CCMe_3)_4(CH_3OH)]3CH_3OH$ (Ln = Gd (1), Tb (2), Dy (3), and Ho (4); Scheme 2). X-ray diffraction quality single crystals for all four complexes were isolated in good yield. The general chemical reaction involved in the formation of complexes 1–4 is summarized in eqn (1):

HL þ Ln NOð $_3$Þ$_3$$nH_2O$ þ 0:5Co_2ðm-OH_2ÞðO$_2$CCMe$_3$Þ$_4$ðHO$_2$CCMe$_3$Þ$_4$ þ 2NEt_3 MeOH! CoLnðm$_2$-LÞðm$_2$-OOCCMe$_3$Þ$_4$ðMeOHÞ3MeOH

þ 2ðNEt_3HÞþ þ Hþ þ 3NO_3 þ H_2O (1)

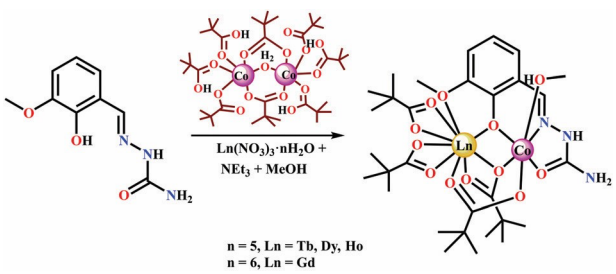

Scheme 2 Synthesis of complexes 1-4 (Ln = Gd (1), Tb (2), Dy (3), and Ho (4)).

The solid-state and single crystalline compounds obtained from the above-mentioned reaction sequence were analyzed by FTIR-ATR and PXRD signatures (Fig. S1 and S2 in the ESI†). As purified compounds are immediately characterized by FTIR-ATR spectra, showing the most prominent Co^{II}-bound imine stretching frequencies within 1607–1609 cm^1 range for all four complexes. The Co^{II}-bound carbonyl (CQO) stretching frequencies from the semicarbazide end appear at 1661–1670 cm^1. The asymmetric stretching frequencies for three different types of binding of pivalate anions to both Co^{II} and Ln^{III} centers are spotted at 1562–1564 cm^1 and the symmetric stretching frequencies appear within 1420–1426 cm^1.

The capping-cum-bridging and aggregation inhibiting roles of the pivalate anions are synergistic in nature in the presence of the L. Coordination-assisted cleavage of Co_2-Piv was crucial for the in situ supply of required numbers of pivalate anions. Use of other

commercially available cobalt(II) salts and external addition of NaPiv failed to reproduce the reported products, confirming the selectivity of the explored reaction path involving Co_2-Piv and 4f metal ion salts. The other ratios of Co_2-Piv and lanthanide nitrate salts were also used to check the reproducibility of this system but either they failed to produce any single crystal or produced the same dimeric unit.

The dimetallic species are formed from the site and donor atom specific coordination of one singly charged and functionally pentadentate L unit, around two different types of metal ions having distinct demand of coordination geometries of individual metal ions.

Description of the crystal structure

Appropriate X-ray quality single crystals of 1-4 were obtained from room-temperature solvent evaporation of the mother liquor at the end of the individual reactions. All four electroneutral complexes are found to be isostructural, and somewhat

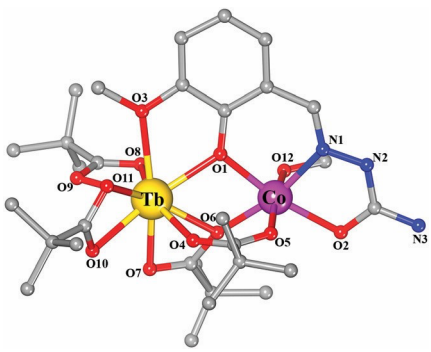

Fig. 1 Molecular structure of complex 2. Hydrogen atoms and solvent molecules are omitted for clarity.

interestingly, all of them crystallize in same orthorhombic space group $Pca2_1$. In all four cases, the asymmetric unit contains the $[CoLn(L)(O_2CCMe^1)_4(CH_3OH)]3CH_3OH$ unit. As all the complexes are structurally similar, a detailed description for the structure of complex 2 (Ln = Tb^{III}) has therefore been considered as a representative one for the entire family. Selected bond distances and angles are collected in Tables S4 and S5 in the ESI.† The perspective view of the structure for 2 is depicted in Fig. 1. The analysis of the X-ray structure exposed that only one L unit is sufficient to hold two different metal ions in two different coordination geometries. The planar ONO part of L is appropriate to bind the Co^{II} centre in the meridional mode. The bridging support from the adjacent bidentate (OO) part was appropriate to hook up the bigger 4f ion along with two chelating and two bridging pivalate ions fulfilling the remaining coordination sites of both the metal ion centres. No solvent-derived HO or O^2 ion was necessary to sustain and stabilize the dinuclear structure. All neutral bimetallic complexes $[CoLn(L)(O_2CCMe_3)_4(CH_3OH)]$ $3CH_3OH$ comprise a nine-coordinated polyhedra around the lanthanide(III) ion and a six-coordinated polyhedra around the cobalt(II) ion. Two polyhedra are triply bridged by ligand phenoxido (O1), m_2-Z^1:Z^1-Piv (O4, O5) and m_2-Z^2:Z^1-Piv (O6) units. The central core of complex 2 was characterized by dissimilar Co–O (Co–O1 and Co–O6, 2.036(5) and 2.092(5) Å), and dissimilar Tb–O (Tb–O1 and Tb–O6, 2.330(5) and 2.431(5) Å) bonds from two different types of O donor atoms (Fig. 2). Interestingly, the Co– O1–Tb angle of 106.32(19)1 for the phenoxido O bridge is wider than the Co–O6–Tb angle of 101.09(18)1 for the O bridge of m_2-Z^2:Z^1-Piv. These two bridges bring CoTb separation at octahedral O_5N coordination environment calculated from SHAPE analysis[22] (Table S2, ESI†), which originated from tridentate (ONO) meridional binding from L, two bridging pivalate anions and one terminal MeOH molecule. The ligand bite forms six- and fivemembered chelate rings having O1–Co–N1 and N1–Co–O2 angles of 89.15(19)1 and 77.52(19)1 respectively in a usual trend. Within the ligand anion plane, the non-chelated O6–Co–O2 angle is obtuse at 114.49(18)1. The apical methanol oxygen (O12) provides the perpendicular angles of 83.95(19)–96.89(19)1 to the ligand– chelated CoO_3N square plane. For the other apical pivalate oxygen (O5), the angles remain within 85.34(18)–93.5(2)1. The bridging phenoxido oxygen (O1) donor from this end connects the adjacent Tb center. Finally, the sixth coordination site is occupied by a terminal MeOH (O12) molecule. Within the O_5N octahedral coordination sphere, the Co–N1 separation is 2.039(5) Å and the remaining Co–O distances span from 2.031(5) to 2.105(5) Å with the longest one for carbonyl oxygen (O2) coordination. The variation in the Co–O bond distances is expected due to the presence of four different types of O donor atoms (Table S4, ESI†). The nine-coordinated Tb^{III} ion remains within an O_9 environment, which can be better visualized as a Muffin-shaped (MFF-9) geometry from continuous SHAPE analysis (Fig. 3). The values for the tricapped trigonal prism (TCTPR-9) and the capped square antiprism (CSAPR-9) geometries are also close to the Muffin geometry (Table S3 in ESI†). The Tb^{III} center is bound to the bidentate and hard O,O donor part of L with enough capping supports from four pivalate anions, originating slowly from Co_2-Piv. The remaining seven positions were occupied by seven O donor centres of four pivalate ions, two of which show the bidentate chelating mode. Third and fourth pivalate ions are forced to bridge the adjacent Co^{II} and Tb^{III} centers in the m_2:Z^1:Z^1 and m_2:Z^2:Z^1 mode. The O6 centre from m_2:Z^2:Z^1 bridging remains in a pyramidal geometry. The release of four pivalate ions from Co_2-Piv is just appropriate in occupying the remaining coordination positions around the Co^{II} and Tb^{III} ions. Nine Tb–O bonds are formed from one bridging phenoxido O donor (Tb–O1, 2.330(5) Å), one terminal ligand –OMe group (Tb–O3, 2.545(5) Å), one m_2-Z^1:Z^1-carboxylato O donor (Tb–O4, 2.271(5) Å), two m_2-Z^2:Z^1-carboxylato O donors (Tb–O6, 2.431(5) Å and Tb–O7, 2.465(5) Å), four Z^2-carboxylato O donors (Tb–O8, 2.422(5) Å, Tb–O9, 2.414(5) Å, Tb–O10, 2.410(5) Å, and Tb–O11, 2.438(5) Å).

[1] .499 Å. The six-coordinate Co^{II} center remained in a distorted

The dimeric unit propagates along one axis via hydrogen bonding between the primary amine and secondary amine groups of the semicarbazide part and the two pivalate oxygen

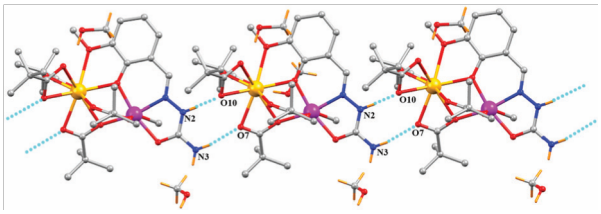

Fig. 4 Hydrogen-bonded connections with amine hydrogen and pivalate oxygen atoms for 1D chain structure in 2.

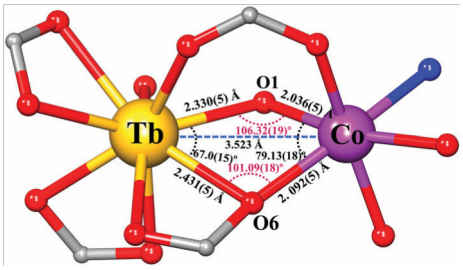

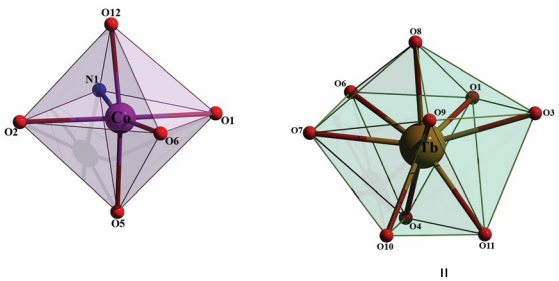

Fig. 3 Distorted octahedral geometry around the Co ion (left); muffinFig. 2 Bond distances and bond angles within the TbO_2Co core. shaped geometry around the Tb^{III} ion (right).

donors of theadjacentmolecule (N2H2O10and N3H3O7) (Fig. 4). The individual CoTb complexes are separated by the solvent MeOH molecules, resulting in intermolecular distances for Co(II)Tb(III), Co(II)Co(II), and Tb(III)Tb(III) at 7.514, 9.766 and 10.198 Å respectively (Fig. S4 in ESI†).

Magnetic properties

Magnetic susceptibility data for complexes 1–4 were measured on polycrystalline samples and the data were collected over the temperature range 2–30 K under an applied direct current magnetic field of 193 Oe and in the range of 2–300 K under a dc field of 3000 Oe. The wT vs. T plot is shown in Fig. 5 (top). At room temperature, the wT values for complexes 1–4 are 10.35, 14.13, 16.21 and 15.93 cm^3 K mol^1 respectively, which is magnitude-wise quite close with the expected values of 10.5,

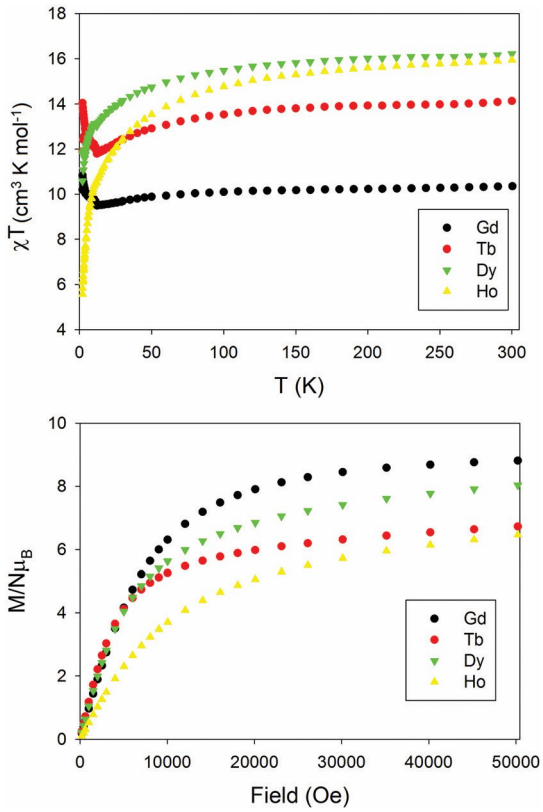

Fig. 5 Plot of wT product vs. Temperature for complexes 1–4 at applied fields of 3000 Oe (2–300 K) (top). Magnetization vs. field plot for the complexes 1–4 (bottom).

14.3, 16.6 and 16.5 cm^3 K mol^1 respectively. The wT values at 300 K are in agreement with the expected theoretical values for one cobalt(II) ion and one lanthanide(III) ion, taking into account the spin-only moment for 1 or strong spin–orbit coupling for 2, 3 and 4. The wT products are mostly constant down to 70 K and below this temperature a decrease is observed in all cases. The observed decrease is as expected due to the strong spin–orbit coupling in all complexes, and in complex 1 it is caused by the Co^{II} ion in a distorted octahedral environment. For 1 and 2 (Gd
and Tb) with a lower temperature, a minimum is reached first and then a sharp increase occurs in the low temperature range. This clearly indicates a ferromagnetic interaction between the Co^{II} and the Ln^{III} ion (Gd in 1 and Tb in 2). For 3 (Ln = Dy), the wT product does not clearly increase in the low temperature range. This can be due to an antiferromagnetic coupling or to the susceptibility data dominated by the depopulation of the M_j sublevels of the lanthanide(III) ions. The magnetization vs. field plot is shown in Fig. 5 (bottom) for all the complexes at 2K show saturation at a non-zero magnetic moment. For 1 (Co–Gd), the saturation magnetization is close to the value of 8.8 Nb expected for one Gd^{III} (S = 7/2) and a Co^{II} (effective spin at 2 K is 1/2) due to large anisotropy on pseudooctahedral coordination geometry of Co(II) ion in the presence of isotropic Gd(III) neighbor ion. Similarly, for complexes 2–4, magnetization initially increases steeply at low fields and then gradually increases with increasing field up to 6.7 Nb for 2, 8.0 Nb for 3 and 6.4 Nb for 4 at 50 kOe and 2 K. For these complexes, there is clearly a magnetic ground state populated at 2 K.

The Co-Ln unit is bridged by one phenoxido group (Co–O–Gd angle 106.401) from the Schiff base ligand anion, one oxygen from pivalate using the syn and anti-positions for the electron pairs (Co–O–Gd 100.701) and one syn,syn-pivalate. Clearly for complexes 1 and 2, the ferromagnetic exchange pathways between Co^{II}–Ln^{III} centers dominate in the magnetic behavior.

Ac magnetic susceptibility data were collected for all complexes at two frequency values (100 and 1500 Hz) and 0 Oe and 2000 Oe dc field values. Only very small tails of out-of-phase ac magnetic susceptibility values were observed for all complexes below 2.2 K. The dinuclear 3d–4f complexes do not show relevant SMM properties with or without an applied dc field.

Conclusions

Synergistic and cooperative coordination of cobalt(II) and selected 4f ions in the +3 oxidation state has been established via exploitation of the selective coordination ability of the ligand anion (L). The exercise led to the availability of four [$Co^{II}Ln^{III}$] complexes. The planar ONO part and the adjacent OO part of the ligand anion accomplish the attraction of distorted octahedral Co^{II} and muffin-shaped nine coordinate Ln^{III} ions having two and seven coordination sites to be occupied by Co_2-Piv-derived pivalate oxygen donors. Trapping of two different types of metal ions in two different coordination geometries and attachment to a single ligand anion frame are responsible for the reciprocally exclusive distortion of individual coordination spheres. The coordination of two different metal ions does not allow much twisting respective chelating parts.

The dc magnetic susceptibility reveals the ferromagnetic exchange interaction for complexes 1 and 2 comprising Gd^{III} and Tb^{III} ions, whereas complexes 3 and 4 containing Dy^{III} and Ho^{III} ions show the antiferromagnetic interaction. All the four complexes were not able to show SMM property in the presence and absence of a dc magnetic field.

Conflicts of interest

There are no conflicts to declare.

Acknowledgements

M. B. is thankful to University Grants Commission (UGC) New Delhi, India for financial support. We are also thankful to the DST, New Delhi, India, for providing the single-crystal X-ray diffractometer facility at the Department of Chemistry, IIT Kharagpur, under its FIST program. ECS acknowledges the financial support from the Spanish Government, (Grant PGC2018-098630-B-I00).

Notes and references

1 (a) C. Benelli and D. Gatteschi, Chem. Rev., 2002, 102, 2369–2387; (b) P. Zhang, Y.-N. Guo and J. Tang, Coord. Chem. Rev., 2013, 257, 1728–1763; (c) B.-W. Wang, S.-D. Jiang, X.-T. Wnag and S. Gao, Sci. China, Ser. B: Chem., 2009, 52, 1739–1758.

2 (a) J.-P. Costes, F. Dahan, A. Dupuis and J.-P. Laurent, Inorg. Chem., 1996, 35, 2400–2402; (b) A. Bhunia, M. T. Gamer, L. Ungur, L. F. Chibotaru, A. K. Powell, Y. Lan, P. W. Roesky, F. Menges, C. Riehn and G. Niedner-Schatteburg, Inorg. Chem., 2012, 51, 9589–9597; (c) M. Andruh, J.-P. Costes, C. Diaz and S. Gao, Inorg. Chem., 2009, 48, 3342–3359; (d) H. L. C. Feltham and S. Brooker, Coord. Chem. Rev., 2014, 276, 1–33; (e) P. Wang, S. Shannigrahi, N. L. Yakovlev and T. S. Andy, Hor, Dalton Trans., 2014, 43, 182–187.

3 (a) M. Holynska, D. Premuzic, I.-R. Jeon, W. Wernsdorfer, R. Clerac and S. Dehnen, Chem. – Eur. J., 2011, 17, 9605–9610; (b) H. Ke, X. Lu, W. Wei, W. Wang, G. Xie and S. Chen, Dalton Trans., 2017, 46, 8138–8145; (c) H. L. C. Feltham, Y. Lan, F. Klçwer, L. Ungur, L. F. Chibotaru, A. K. Powell and S. Brooker, Chem. – Eur. J, 2011, 17, 4362–4365.

4 (a) R. Sessoli and A. K. Powell, Coord. Chem. Rev., 2009, 253, 2328–2341; (b) C. M. Zaleski, E. C. Depperman, J. W. Kampf, M. L. Kirk and V. L. Pecoraro, Angew. Chem., Int. Ed., 2004, 43, 3912–3914; (c) S. Osa, T. Kido, N. Matsumoto, N. Re, A. Pochaba and J. Mrozinski, J. Am. Chem. Soc., 2004, 126, 420–421; (d) X.-C. Huang, C. Zhou, H.-Y. Wei and X.-Y. Wang, Inorg. Chem., 2013, 52, 7314–7316.

5 (a) A. Candini, S. Klyatskaya, M. Ruben, W. Wernsdorfer and M. Affronte, Nano Lett., 2011, 11, 2634–2639; (b) D. Gatteschi, R. Sessoli and J. Villain, Molecular Nanomagnets, Oxford University Press, Oxford, UK, 2006.

6 (a) M. Urdampilleta, S. Klyatskaya, J.-P. Cleuziou, M. Ruben and W. Wernsdorfer, Nat. Mater., 2011, 10, 502–506; (b) L. Bogani and W. Wernsdorfer, Nat. Mater., 2008, 7, 179–186.

7 (a) R. Sessoli, D. Gatteschi, A. Caneschi and M. A. Novak, Nature, 1993, 365, 141–143; (b) M. N. Leuenberger and D. Loss, Nature, 2001, 410, 789–793; (c) E. Coronado and A. J. Epsetin, J. Mater. Chem., 2009, 19, 1670–1671.

8 (a) K. Griffiths, P. Kumar, G. R. Akien, N. F. Chilton, A. Abdul-Sada, G. J. Tizzard, S. J. Coles and G. E. Kostakis, Chem. Commun., 2016, 52, 7866–7869; (b) K. Griffiths, P. Kumar, J. D. Mattock, A. Abdul-Sada, M. B. Pitak, S. J. Coles, O. Navarro, A. Vargas and G. E. Kostakis, Inorg. Chem., 2016, 55, 6988–6994.

9 (a) Y.-Z. Zheng, M. Evangelisti, F. Tuna and R. E. P. Winpenny, J. Am. Chem. Soc., 2012, 134, 1057–1065; (b) C.-M. Liu, D.-Q. Zhang and D.-B. Zhu, RSC Adv., 2014, 4, 53870–53876; (c) G. Karotsis, S. Kennedy, S. J. Teat, C. M. Beavers, D. A. Fowler, J. J. Morales, M. Evangelisti, S. J. Dalgarno and E. K. Brechin, J. Am. Chem. Soc., 2010, 132, 12983–12990; (d) Y.-Z. Zheng, M. Evangelisti and R. E. P. Winpenny, Chem. Sci., 2011, 2, 99–102.

10 (a) H. Ke, L. Zhao, Y. Guo and J. Tang, Dalton Trans., 2012, 41, 2314–2319; (b) S. K. Langley, B. Moubaraki and K. S. Murray, Dalton Trans., 2010, 39, 5066–5069; (c) A. J. Blake, R. O. Gould, P. E. Y. Milne and R. E. P. Winpenny, J. Chem. Soc., Chem. Commun., 1991, 1453–1455; (d) F. Pointillart, K. Bernot, R. Sessoli and D. Gatteschi, Chem. – Eur. J., 2007, 13, 1602–1609; (e) V. Baskar, K. Gopal, M. Helliwell, F. Tuna, W. Wernsdorfer and R. E. P. Winpenny, Dalton Trans., 2010, 39, 4747–4750; (f) E. Colacio, J. Ruiz, E. Ruiz, E. Cremades, J. Krzystek, S. Carretta, J. Cano, T. Guidi, W. Wernsdorfer and E. K. Brechin, Angew. Chem., Int. Ed., 2013, 52, 9130–9134; (g) S. K. Langley, D. P. Wielechowski, B. Moubaraki and K. S. Murray, Chem. Commun., 2016, 52, 10976–10979.

11 D. Basak, J. V. Leusen, T. Gupta, P. Ko¨gerler, V. Bertolasi and D. Ray, Inorg. Chem., 2020, 59, 2387–2405.

12 (a) F.-X. Shen, H.-Q. Li, H. Miao, D. Shao, X.-Q. Wei, L. Shi, Y.-Q. Zhang and X.-Y. Wang, Inorg. Chem., 2018, 57, 15526–15536; (b) J.-W. Yang, Y.-M. Tian, J. Tao, P. Chen, H.-F. Li, Y.-Q. Zhang, P.-F. Yan and W.-B. Sun, Inorg. Chem., 2018, 57, 8065–8077; (c) A. Das, S. Goswami, R. Sen and A. Ghosh, Inorg. Chem., 2019, 58, 5787–5798; (d) V. Chandrasekhar, B. M. Pandian, R. Azhakar, J. J. Vittal and R. Cle´rac, Inorg. Chem., 2007, 46, 5140–5142; (e) M. Dolai, M. Ali, J. Titisˇ and R. Bocˇa, Dalton Trans., 2015, 44, 13242–13249.

13 (a) M. Li, H. Wu, S. Zhang, L. Sun, H. Ke, Q. Wei, G. Xie, S. Chen and S. Gao, Eur. J. Inorg. Chem., 2017, 811–819; (b) M. Li, H. Wu, Q. Wei, H. Ke, B. Yin, S. Zhang, X. Lv, G. Xie and S. Chen, Dalton Trans., 2018, 47, 9482–9491; (c) H. Wu, M. Li, S. Zhang, H. Ke, Y. Zhang, G. Zhuang, W. Wang, Q. Wei, G. Xie and S. Chen, Inorg. Chem., 2017, 56, 11387–11397.

14 G. AromI`, A. S. Batsanov, P. Christian, M. Helliwell, A. Parkin, S. Parsons, A. A. Smith, G. A. Timco and R. E. P. Winpenny, Chem. – Eur. J., 2003, 9, 5142–5161.

15 SAINT Plus, Version 7.03, Bruker AXS Inc., Madison, WI, 2004.

16 Smart and XPREP, Siemens Analytical X-ray Instruments Inc., Madison, WI, 1995.

17 G. M. Sheldrick, SHELXT-Integrated Space-Group and Crystal-Structure Determination, Acta Crystallogr., Sect. A: Found. Adv., 2015, 71, 3–8.

18 G. M. Sheldrick, Crystal Structure Refinement with SHELXL, Acta Crystallogr., Sect. C: Struct, Chem, 2015, 71, 3–8.

19 O. V. Dolomanov, L. J. Bourhis, R. J. Gildea, J. A. K. Howard and H. Puschmann, OLEX2: a complete structure solution, refinement and analysis program, J. Appl. Crystallogr., 2009, 42, 339–341.

20 G. M. Sheldrick, SADABS: Software for empirical absorption correction, Ver. 2.05, University of Go¨ttingen, Go¨ttingen, Germany, 2002.

21 DIAMOND, Visual Crystal Structure Information System, version 3.1, Crystal Impact, Bonn, Germany, 2004.

22 (a) S. Alvarez, P. Alemany, D. Casanova, J. Cirera, M. Llunell and D. Avnir, Coord. Chem. Rev., 2005, 249, 1693–1708; (b) D. Casanova, J. Cirera, M. Liunell, P. Alemany, D. Avnir and S. Alvarez, J. Am. Chem. Soc., 2004, 126, 1755–1763.